



# Energy-Efficient Optimization for Joint Design of Power Allocation and Beamforming in Downlink mmWave Communication Systems with NOMA

Jiali Cai<sup>1</sup>(✉) , Xiangbin Yu<sup>1,2</sup> , Xu Huang<sup>1</sup>, and Cuimin Pan<sup>1</sup>

<sup>1</sup> College of Electronic and Information Engineering, Nanjing University of Aeronautics and Astronautics, Nanjing 210016, China

<sup>2</sup> Key Laboratory of Wireless Sensor Network and Communication, Shanghai Institute of Microsystem and Information Technology, Chinese Academy of Sciences, Shanghai, China

**Abstract.** In this paper, we develop two energy-efficient joint power allocation (PA) and beamforming (BF) design schemes for a two-user downlink millimeter-wave system with non-orthogonal multiple access under imperfect channel state information. The optimization problem is formulated by considering the maximum power and minimum rate constraints. Specifically, by means of block coordinate descent algorithm, the problem is transformed into two sub-problems: PA problem and BF problem. First, we derive a closed-form optimal PA solution for each iteration of concave-convex procedure so as to obtain a suboptimal PA scheme for the fixed BF. With this PA scheme, two suboptimal BF schemes are proposed based on successive convex approximation and one-dimensional search method, respectively. Simulation results validate the rational of two proposed schemes and show that the former scheme can achieve higher energy efficiency while the latter has small performance loss but lower complexity.

**Keywords:** Millimeter-wave · Non-orthogonal multiple access · Imperfect channel state information · Energy efficiency · Power allocation · Beamforming

## 1 Introduction

With the rapid development of mobile communications, spectrum resource shortage brings great challenges to existing technologies. Thus, a promising multiple

---

Supported by the Fundamental Research Funds for the Central Universities of NUAU (No. kfjj20200414), Natural Science Foundation of Jiangsu Province in China (No. BK20181289) and Open Research Fund Key Laboratory of Wireless Sensor Network and Communication of Chinese Academy of Sciences (2017006).

access technique, non-orthogonal multiple access (NOMA) has been proposed. NOMA adopts non-orthogonal transmission at the sender, actively introduces interference information, and realizes correct demodulation at the receiver by successive interference cancellation [1]. Besides, due to the large and available bandwidth, millimeter-wave (mmWave) communication is expected to support high data rates.

Therefore, in order to take advantage of both technologies, the studies about the combination of mmWave and NOMA have received more attention [2–8]. In [2] and [3], a joint beamforming (BF) and power allocation (PA) problem was formulated to maximize the sum rate for uplink and downlink mmWave-NOMA system respectively under perfect channel state information (CSI). Different from the studies above that focused on the spectral efficiency, [4] explored the energy-efficient PA problem for uplink mmWave-NOMA system, while [5] investigated the similar problem for downlink system. [6] studied mmWave-NOMA uplink systems and considered the fairness of the energy efficiency (EE) optimization problem. Combining with the mmWave channel estimation, the authors firstly used the analog BF scheme based on discrete Fourier transform codebook, and then put forward to a two-loop iterative algorithm for joint PA and digital BF design scheme of resource allocation. However, they didn't consider about the joint optimization problem since the analog BF vectors were selected by codebooks in the papers. In [7], a joint PA and BF scheme was developed so as to maximize the EE for downlink mmWave-NOMA system. And in [8], the authors proposed two beamwidth control methods and analyzed the energy-efficient digital precoder design by adopting a NOMA user scheduling algorithm for downlink mmWave-NOMA system.

Most of the existing works assume the perfect CSI is available, however, it can not be guaranteed in practice. Hence, we propose two schemes of joint PA and BF design for maximizing EE with imperfect CSI in the downlink mmWave-NOMA system. The main contributions in this paper are summarized as follows:

- With imperfect CSI, the EE maximization problem for two-user downlink mmWave-NOMA is formulated. The original optimization problem, which is difficult to solve directly, can be decomposed into two sub-problems. One is the PA problem and the other is the BF design problem. Then an efficient iterative algorithm via the block coordinate descent (BCD) method is developed.
- For the fixed BF, we address the PA problem by means of concave-convex procedure (CCCP). Moreover, the closed-form optimal solution for each iteration of CCCP is derived with the aid of Lambert W function. For the fixed PA, we adopt successive convex approximation (SCA) to obtain a suboptimal solution, and derive another low-complexity suboptimal solution by one-dimensional (1D) search method. The simulation shows that the former can achieve better EE performance, and the latter has better computational efficiency.

Notations:  $(\cdot)^T$  and  $(\cdot)^H$  stand for the transpose, conjugate transpose, respectively.  $|\cdot|$  and  $\|\cdot\|$  are absolute value and value of two-norm, respectively. Vectors

and matrices are respectively represented by boldface lower and upper case symbols,  $\mathbf{I}_N$  is an  $N \times N$  identity matrix.  $\mathcal{CN}(\mathbf{0}, \mathbf{R})$  denotes the complex Gaussian distribution with zero-mean and covariance matrix  $\mathbf{R}$ .

## 2 System Model and Problem Formulation

### 2.1 System Model

Considering a two-user downlink mmWave-NOMA system similar to that in [7], we assume that the base station (BS) is equipped with a radio frequency (RF) chain and  $N$ -element antenna array to support two single-antenna users. Each antenna branch of the BS has a phase shifter and a low-noise amplifier (LNA). All LNAs have the same scaling factor, therefore, the  $N$  dimensional BF vector  $\mathbf{w}$  has constant-modulus (CM) elements, namely  $|\mathbf{w}_n| = 1/\sqrt{N}$ ,  $n = 1, 2, \dots, N$ . The mmWave channel between the BS and  $i$ -th user ( $i = 1, 2$ ) with perfect CSI can be modeled as  $\mathbf{h}_i = \sum_{l=1}^{L_i} \lambda_{i,l} \mathbf{a}(N, \theta_{i,l})$ , where  $L_i$ ,  $\lambda_{i,l}$  and  $\theta_{i,l}$  indicate the number of channel paths, complex gain and the angle of departure (AoD) of the  $l$ -th path between the BS and User- $i$ , respectively, and  $\mathbf{a}(N, \theta) = [e^{j\pi 0 \cos \theta}, e^{j\pi 1 \cos \theta}, \dots, e^{j\pi(N-1) \cos \theta}]^T$  is the steering vector function [2–5, 7]. In view of the difficulty of obtaining perfect CSI, we consider imperfect CSI at the BS. According to [9], the mmWave channel for the  $i$ -th user with imperfect CSI can be expressed as

$$\mathbf{h}_i = \hat{\mathbf{h}}_i + \sqrt{1 - \rho} \tilde{\mathbf{h}}_i, \quad (1)$$

where  $\hat{\mathbf{h}}_i$  denotes the estimated channel vector,  $\rho$  denotes the CSI accuracies of the non-line-of-sight (NLOS) components,  $\tilde{\mathbf{h}}_i \sim \mathcal{CN}(\mathbf{0}, \mathbf{I}_N)$ . Therefore, the received signal of User- $i$  can be expressed as

$$\begin{aligned} \mathbf{y}_i &= \hat{\mathbf{h}}_i^H \mathbf{w} \sqrt{p_1} x_1 + \hat{\mathbf{h}}_i^H \mathbf{w} \sqrt{p_2} x_2 \\ &+ \sqrt{1 - \rho} \tilde{\mathbf{h}}_i^H \mathbf{w} \sqrt{p_1} x_1 + \sqrt{1 - \rho} \tilde{\mathbf{h}}_i^H \mathbf{w} \sqrt{p_2} x_2 + \mathbf{n}_i, \end{aligned} \quad (2)$$

where  $x_i$  is the transmission signal of User- $i$ ,  $p_i$  denotes the transmission power and  $\mathbf{n}_i$  denotes the Gaussian white noise with  $\mathcal{CN}(\mathbf{0}, \sigma^2 \mathbf{I}_N)$ .

### 2.2 Problem Formulation

For the above system, we need to consider two cases of decoding orders:

Case-1: The signal of User-1  $x_1$  is decoded first by regarding the signal of User-2  $x_2$  as interference, then  $x_2$  is decoded after removing  $x_1$ . In this case, the achievable rates of two users are given as

$$\begin{cases} R_1^{(1)} = \log_2 \left( 1 + \frac{\hat{c}_1 p_1}{\hat{c}_1 p_2 + q(p_1 + p_2) + \sigma^2} \right) \\ R_2^{(1)} = \log_2 \left( 1 + \frac{\hat{c}_2 p_2}{q(p_1 + p_2) + \sigma^2} \right) \end{cases}, \quad (3)$$

where  $q = 1 - \rho$  and  $\hat{c}_i = \left| \hat{\mathbf{h}}_i^H \mathbf{w} \right|^2$ ,  $i = 1, 2$ , in which the implicit assumption is  $\hat{c}_1 \leq \hat{c}_2$ .

Case-2: The signal of User-2  $x_2$  is decoded first. In this case, the achievable rates of two users are given as

$$\begin{cases} R_1^{(2)} = \log_2 \left( 1 + \frac{\hat{c}_1 p_1}{q(p_1 + p_2) + \sigma^2} \right) \\ R_2^{(2)} = \log_2 \left( 1 + \frac{\hat{c}_2 p_2}{\hat{c}_2 p_1 + q(p_1 + p_2) + \sigma^2} \right) \end{cases}. \quad (4)$$

Similarly, the implicit assumption is  $\hat{c}_1 \geq \hat{c}_2$ .

Therefore, the EE optimization problem in both cases with imperfect CSI is formulated as

$$\begin{aligned} \max_{p_1, p_2, \mathbf{w}} \quad & \eta_{EE}^{(j)} = \frac{R_1^{(j)} + R_2^{(j)}}{\xi(p_1 + p_2) + P_C} \\ \text{s.t.} \quad & R_i^{(j)} \geq r_i, i = 1, 2, \\ & p_1 + p_2 \leq P_{\max}, \\ & |[\mathbf{w}]_n| = \frac{1}{\sqrt{N}}, n = 1, 2, \dots, N, \end{aligned} \quad (5)$$

where  $\eta_{EE}^{(j)}$  is the system EE in Case- $j$ ,  $r_i$  is the minimum rate of User- $i$ ,  $P_{\max}$  is the maximum transmission power at the BS and  $\xi$  denotes the coefficient of LNAs.  $P_C$  is the fixed circuit power consumption, which can be expressed as  $P_C = P_{BB} + P_{RF} + NP_{PS} + NP_{LNA}$ , in which  $P_{BB}, P_{RF}, P_{PS}, P_{LNA}$  are the power consumption of the baseband, the RF chain, the phase shifter and LNA, respectively.

### 3 Joint PA and BF Design Schemes

This section presents two schemes of joint PA and BF design. Due to the limited space, we only consider about the optimization problem in Case-2 under imperfect CSI, and that in Case-1 can be solved by using the similar algorithms. The superscript  $(j)$  in  $\eta_{EE}^{(j)}$  and  $R_i^{(j)}$  is omitted for the sake of discussion. Obviously, due to the non-concave objective function as well as the coupled optimization variables, the optimization problem (5) is difficult to solve directly. Therefore, we introduce a new variable  $P = p_1 + p_2$ , so that  $p_2$  can be replaced as  $P - p_1$ , then (5) can be transformed into

$$\begin{aligned} \max_{p_1, P, \mathbf{w}} \quad & \eta_{EE} = \frac{\log_2 \left( \left( 1 + \frac{\hat{c}_1 p_1}{qP + \sigma^2} \right) \left( 1 + \frac{\hat{c}_2 (P - p_1)}{\hat{c}_2 p_1 + qP + \sigma^2} \right) \right)}{\xi P + P_C} \\ \text{s.t.} \quad & \hat{c}_2 (P - p_1) \geq \phi_2 (\hat{c}_2 p_1 + qP + \sigma^2), \\ & \hat{c}_1 p_1 \geq \phi_1 (qP + \sigma^2), \\ & 0 \leq P \leq P_{\max}, \\ & |[\mathbf{w}]_n| = \frac{1}{\sqrt{N}}, n = 1, 2, \dots, N, \\ & \hat{c}_1 \geq \hat{c}_2, \end{aligned} \quad (6)$$

where  $\phi_i = 2^{r_i} - 1, i = 1, 2$ . According to the first derivative of the objective function in (6) with respect to  $p_1$  and  $\hat{c}_1 \geq \hat{c}_2$ , we can get  $\partial\eta_{EE}/\partial p_1 \geq 0$ , i.e.,  $\eta_{EE}$  is monotonically increasing with respect to  $p_1$ . Thus, the optimal  $p_1$  is its upper bound, which can be obtained by the rate constraint of User-2:

$$p_1^* = \frac{\hat{c}_2 P - \phi_2 (qP + \sigma^2)}{(\phi_2 + 1) \hat{c}_2}. \quad (7)$$

With  $p_1^*$ ,  $p_2$  can be rewritten as  $P - p_1^*$  and (6) can be reduced to the following problem with respect to  $\{P, \mathbf{w}\}$ :

$$\begin{aligned} \max_{P, \mathbf{w}} \quad & J = \frac{\log_2 \left( \frac{(\hat{c}_1 \hat{c}_2 + q(\phi_2 + 1) \hat{c}_2 - \phi_2 \hat{c}_1 q) P + \sigma^2 ((\phi_2 + 1) \hat{c}_2 - \phi_2 \hat{c}_1)}{(qP + \sigma^2) \hat{c}_2} \right)}{\xi P + P_C} \\ \text{s.t.} \quad & \hat{c}_1 \frac{\hat{c}_2 P - \phi_2 (qP + \sigma^2)}{(\phi_2 + 1) \hat{c}_2} \geq \phi_1 (qP + \sigma^2), \\ & 0 \leq P \leq P_{\max}, \\ & |[\mathbf{w}]_n| = \frac{1}{\sqrt{N}}, n = 1, 2, \dots, N, \\ & \hat{c}_1 \geq \hat{c}_2, \end{aligned} \quad (8)$$

We can observe from (8) that when one of  $P$  and  $\mathbf{w}$  is fixed, the resultant problem can be efficiently solved. Therefore, we adopt the BCD algorithm to solve this optimization problem. In particular, we decompose the problem (8) into PA problem and BF design problem, and then solve the PA problem for given  $\mathbf{w}$ , and solve the BF design problem for given  $P$ .

### 3.1 Solution of PA Problem

For any feasible  $\mathbf{w}$ , the PA problem in (8) can be formulated as

$$\begin{aligned} \max_P \quad & J \\ \text{s.t.} \quad & P_{\min} \leq P \leq P_{\max}, \end{aligned} \quad (9)$$

where  $P_{\min} = \frac{\phi_1(\phi_2+1)\hat{c}_2\sigma^2 + \hat{c}_1\phi_2\sigma^2}{\hat{c}_1\hat{c}_2 - \hat{c}_1\phi_2q - \phi_1(\phi_2+1)\hat{c}_2q}$ , which is obtained by the rate constraint of User-1. Besides, the numerator of  $J$  can be rewritten as  $f_1(P) - f_2(P)$ , where  $f_1(P) = \log_2 \left( (\hat{c}_1 + q(\phi_2 + 1) - \frac{\hat{c}_1\phi_2q}{\hat{c}_2}) P + \sigma^2 \left( (\phi_2 + 1) - \frac{\phi_2\hat{c}_1}{\hat{c}_2} \right) \right)$ ,  $f_2(P) = \log_2 (qP + \sigma^2)$ . Since  $f_1(P)$  and  $f_2(P)$  are convex, we can use CCCP to solve the difference of convex problem. By adopting first-order Taylor expansion at the initial point  $P_0$ ,  $f_2(P)$  is linearized as

$$f_2(P) = \log_2 (qP_0 + \sigma^2) + \frac{q}{\ln 2 (qP_0 + \sigma^2)} (P - P_0). \quad (10)$$

With (10), the optimization problem (9) for given  $P_0$  can be transformed into

$$\begin{aligned} \max_P \quad & J_1 = \frac{\log_2(aP + b) - cP - d}{\xi P + P_C} \\ \text{s.t.} \quad & P_{\min} \leq P \leq P_{\max}, \end{aligned} \quad (11)$$

where

$$\begin{cases} a = \hat{c}_2 \hat{c}_1 + q(\phi_2 + 1)\hat{c}_2 - \phi_2 \hat{c}_1 q \\ b = \sigma^2 ((\phi_2 + 1)\hat{c}_2 - \phi_2 \hat{c}_1) \\ c = \frac{q}{\ln 2(qP_0 + \sigma^2)} \\ d = \log_2 ((qP_0 + \sigma^2) \hat{c}_2) - \frac{q}{\ln 2(qP_0 + \sigma^2)} P_0 \end{cases}. \quad (12)$$

With the aid of Lambert W function  $W(\cdot)$  [10], the solution of  $\partial J_1 / \partial P = 0$  is expressed as

$$\tilde{P} = \frac{1}{a} \left( \frac{\frac{aP_C}{\xi} - b}{W\left(\frac{\frac{aP_C}{\xi} - b}{\exp\left(\left(d - \frac{cP_C}{\xi}\right) \ln 2 + 1\right)}\right)} - b \right). \quad (13)$$

Then, the optimal solution of (12) is given by

$$\begin{cases} P^* = \min \left\{ P_{\max}, \max \left\{ P_{\min}, \tilde{P} \right\} \right\} \\ p_1^* = \frac{\hat{c}_2 P^* - \phi_2 (qP^* + \sigma^2)}{(\phi_2 + 1)\hat{c}_2}, p_2^* = P^* - p_1^* \end{cases}. \quad (14)$$

Therefore, we calculate (14) iteratively by CCCP and obtain the converged solution as a suboptimal solution of (9). The algorithm for PA is summarized as **Algorithm 1**.

---

**Algorithm 1.** CCCP-based PA Algorithm

---

- 1: **Initialize:** tolerances  $\epsilon_1 > 0$ , the number of iterations  $q = 0$  and initial point  $P^{(q)}$ .
  - 2: **repeat**
  - 3:   Update  $P_0 = P^{(q)}$ .
  - 4:    $q = q + 1$ .
  - 5:   Compute  $P^{(q)}, p_1^{(q)}$  according to (14).
  - 6: **until**  $\left| P^{(q)} - P_0 \right| \leq \epsilon_1$
  - 7: **Output:**  $\hat{P}^* = P^{(q)}, \hat{p}_1^* = p_1^{(q)}, \hat{p}_2^* = P^* - p_1^*$ .
- 

### 3.2 Solution of BF Design Problem

For a given  $P$ , the BF problem in (8) can be expressed as

$$\begin{aligned} \max_{\mathbf{w}} \quad & J_2(\mathbf{w}) = \left| \hat{\mathbf{h}}_1^H \mathbf{w} \right|^2 P - \phi_2 (qP + \sigma^2) \frac{\left| \hat{\mathbf{h}}_1^H \mathbf{w} \right|^2}{\left| \hat{\mathbf{h}}_2^H \mathbf{w} \right|^2} \\ \text{s.t.} \quad & \left| \hat{\mathbf{h}}_2^H \mathbf{w} \right|^2 \leq \left| \hat{\mathbf{h}}_1^H \mathbf{w} \right|^2, \\ & |[\mathbf{w}]_n| = \frac{1}{\sqrt{N}}, n = 1, 2, \dots, N. \end{aligned} \quad (15)$$

Let  $\mathbf{H}_i = \hat{\mathbf{h}}_i \hat{\mathbf{h}}_i^H, i = 1, 2$ , and introduce new auxiliary variables  $t_1, t_2$ , then the BF problem can be relaxed to the following problem:

$$\begin{aligned}
 & \max_{\mathbf{w}, t_1, t_2} && t_1 \\
 & \text{s.t.} && 1 \leq \frac{\mathbf{w}^H \mathbf{H}_1 \mathbf{w}}{\mathbf{w}^H \mathbf{H}_2 \mathbf{w}} \leq t_2 \\
 & && \mathbf{w}^H \mathbf{H}_1 \mathbf{w} \geq \frac{t_1 + \phi_2 (qP + \sigma^2) t_2}{P} \\
 & && |[\mathbf{w}]_n| \leq \frac{1}{\sqrt{N}}, n = 1, 2, \dots, N.
 \end{aligned} \tag{16}$$

In what follows, we adopt SCA method to address the problem (16). Accordingly, we need to solve the following convex optimization problem at the  $l$ -th iteration of SCA:

$$\begin{aligned}
 & \max_{\mathbf{w}, t_1, t_2} && t_1 \\
 & \text{s.t.} && 2\text{Re} \{ \mathbf{w}_0^H \mathbf{H}_2 \mathbf{w} \} - \mathbf{w}_0^H \mathbf{H}_2 \mathbf{w} \geq \frac{\mathbf{w}^H \mathbf{H}_1 \mathbf{w}}{t_2}, \\
 & && 2\text{Re} \{ \mathbf{w}_0^H \mathbf{H}_1 \mathbf{w} \} - \mathbf{w}_0^H \mathbf{H}_1 \mathbf{w} \geq \mathbf{w}^H \mathbf{H}_2 \mathbf{w}, \\
 & && 2\text{Re} \{ \mathbf{w}_0^H \mathbf{H}_1 \mathbf{w} \} - \mathbf{w}_0^H \mathbf{H}_1 \mathbf{w} \geq \frac{t_1 + \phi_2 (qP + \sigma^2) t_2}{P}, \\
 & && |[\mathbf{w}]_n| \leq \frac{1}{\sqrt{N}}, n = 1, 2, \dots, N,
 \end{aligned} \tag{17}$$

where  $\mathbf{w}_0 = \mathbf{w}^{(l-1)}$  denotes the value of  $\mathbf{w}$  at the  $(l - 1)$ -th iteration of SCA. Hence, CVX tool is used to obtain a suboptimal solution  $\mathbf{w}^*$  of (15) [11]. To satisfy the CM constraint, we make the CM normalization for each element of  $\mathbf{w}^*$  as follows:

$$[\mathbf{w}^*]_n = \frac{[\mathbf{w}^*]_n}{\sqrt{N} |[\mathbf{w}^*]_n|}, n = 1, \dots, N. \tag{18}$$

As a result, we summarize the first joint design scheme in **Algorithm 2**. Furthermore, due to the poor calculation efficiency of CVX, we propose another scheme to address the BF design problem. When  $p_1, p_2$  is known, the BF problem decomposed from the optimization problem (6) is reduced to

$$\mathcal{L}(\mathbf{w}) = \left( \frac{P}{qP + \sigma^2} - \frac{p_2}{\hat{c}_2 p_1 + qP + \sigma^2} \right) \hat{c}_1 + \frac{p_2}{\hat{c}_2 p_1 + qP + \sigma^2} \hat{c}_2. \tag{19}$$

Let  $\alpha = \frac{p_2}{\hat{c}_2 p_1 + qP + \sigma^2}, \beta = \alpha \frac{qP + \sigma^2}{P}$ , then  $\mathcal{L}(\mathbf{w})$  can be rewritten as

$$\mathcal{L}(\mathbf{w}) = \frac{P}{qP + \sigma^2} [(1 - \beta) \hat{c}_1 + \beta \hat{c}_2]. \tag{20}$$

**Algorithm 2.** Joint PA and BF Algorithm with SCA

---

**Initialize:** tolerances  $\epsilon_2, \epsilon_3 > 0$ , the number of iterations  $t = 0$ , and  $\{P^{(t)}, \mathbf{w}^{(t)}\}$ .

**repeat**

$t = t + 1$ .

Initialize the number of iterations  $l = 0$  and initial point  $\mathbf{w}^{(l)} = \mathbf{w}^{(t)}$ .

**repeat**

$l = l + 1$ .

Calculate the optimal solution  $\mathbf{w}^*$  by (17), (18).

Update  $\mathbf{w}^{(l)} = \mathbf{w}^*$ .

**until**  $\|\mathbf{w}^{(l)} - \mathbf{w}^{(l-1)}\| \leq \epsilon_2$

Update  $\mathbf{w}^{(t)} = \mathbf{w}^{(l)}$ .

Calculate  $P^*$  by **Algorithm 1**.

Update  $P^{(t)} = P^*$ .

**until**  $\|\mathbf{w}^{(t)} - \mathbf{w}^{(t-1)}\| + |P^{(t)} - P^{(t-1)}| \leq \epsilon_3$

**Output:**  $\hat{\mathbf{w}}^* = \mathbf{w}^{(t)}, \hat{P}^* = P^{(t)}, \hat{p}_1^*, \hat{p}_2^*$ .

---

Since  $\hat{c}_i = \mathbf{w}^H \hat{\mathbf{h}}_i \hat{\mathbf{h}}_i^H \mathbf{w}$ ,  $i = 1, 2$ , without considering the constraint of minimum rate, the BF problem can be formulated as

$$\begin{aligned}
 \max_{\mathbf{w}} \quad & J_3(\mathbf{w}) = \mathbf{w}^H \left[ \sqrt{(1-\beta)} \hat{\mathbf{h}}_1 \hat{\mathbf{h}}_1^H + \sqrt{\beta} \hat{\mathbf{h}}_2 \hat{\mathbf{h}}_2^H \right] \mathbf{w} \\
 \text{s.t.} \quad & \left| \hat{\mathbf{h}}_2^H \mathbf{w} \right|^2 \leq \left| \hat{\mathbf{h}}_1^H \mathbf{w} \right|^2, \\
 & |[\mathbf{w}]_n| = \frac{1}{\sqrt{N}}, n = 1, 2, \dots, N.
 \end{aligned} \tag{21}$$

To achieve the maximum  $J_3(\mathbf{w})$ , we first introduce the **Lemma 1**.

**Lemma 1.** *Given  $a_1, a_2 > 0$ , the following inequality holds*

$$a_1 |b_1|^2 + a_2 |b_2|^2 \geq |\sqrt{a_1} b_1 + \sqrt{a_2} b_2|^2 / 2 \tag{22}$$

*Proof.* Since  $a_1, a_2 > 0$ , we can get

$$|\sqrt{a_1} b_1 - \sqrt{a_2} b_2|^2 \geq 0. \tag{23}$$

Expanding (23), we can obtain

$$a_1 |b_1|^2 + a_2 |b_2|^2 \geq 2\sqrt{a_1 a_2} \text{Re}(b_1 b_2^*). \tag{24}$$

Then we have

$$\begin{aligned}
 2 \left( a_1 |b_1|^2 + a_2 |b_2|^2 \right) & \geq a_1 |b_1|^2 + a_2 |b_2|^2 + 2\sqrt{a_1 a_2} \text{Re}(b_1 b_2^*) \\
 & = |\sqrt{a_1} b_1 + \sqrt{a_2} b_2|^2
 \end{aligned} \tag{25}$$

Therefore the inequality (22) holds.

By using the **Lemma 1**, the problem (21) can be transformed into

$$\begin{aligned}
 \max_{\mathbf{w}} \quad & J_4(\mathbf{w}) = \left| \sqrt{(1-\beta)}\hat{\mathbf{h}}_1^H \mathbf{w} + \sqrt{\beta}\hat{\mathbf{h}}_2^H \mathbf{w} \right| \\
 \text{s.t.} \quad & \left| \hat{\mathbf{h}}_2^H \mathbf{w} \right|^2 \leq \left| \hat{\mathbf{h}}_1^H \mathbf{w} \right|^2, \\
 & |[\mathbf{w}]_n| = \frac{1}{\sqrt{N}}, n = 1, 2, \dots, N.
 \end{aligned} \tag{26}$$

And a suboptimal solution can be obtained as

$$\mathbf{w}^* = \frac{1}{\sqrt{N}} \exp \left( j \angle \left\{ \sqrt{(1-\beta)}\hat{\mathbf{h}}_1 + \sqrt{\beta}\hat{\mathbf{h}}_2 \right\} \right). \tag{27}$$

Due to  $\alpha \leq \frac{P}{qP+\sigma^2}$ , we can obtain  $\beta$  belongs to  $[0,1]$ . Moreover, in order to find the optimal solution  $\beta^*$  corresponds to the maximum objective function of the original problem under the given  $p_1, p_2$ , we use the 1D search method, namely  $\beta^* = \arg \max_{\beta \in [0,1]} \mathcal{L}(\mathbf{w})$ . In particular, the BF scheme in [7] is a special case of this proposed scheme when  $\rho = 1$ .

Based on the analysis above, the second suboptimal joint design scheme is summarized as **Algorithm 3**.

---

**Algorithm 3.** Joint PA and BF Algorithm with 1D search

---

**Initialize:** tolerances  $\epsilon_3 > 0$ , the number of iterations  $t = 0$ , and  $\{P^{(0)}, \mathbf{w}^{(0)}\}$ , calculate  $p_1^{(0)}, p_2^{(0)}$  by (14)

**repeat**

$t = t + 1$ .

Calculate  $\beta^* = \arg \max_{\beta \in [0,1]} \mathcal{L}(\mathbf{w})$

Calculate  $\mathbf{w}^*$  with  $\beta^*$  by (22).

Update  $\mathbf{w}^{(t)} = \mathbf{w}^*$ .

Calculate  $P^*, p_1^*, p_2^*$  by **Algorithm 1**.

Update  $P^{(t)} = P^*, p_1^{(t)} = p_1^*, p_2^{(t)} = p_2^*$ .

**until**  $\left\| \mathbf{w}^{(t)} - \mathbf{w}^{(t-1)} \right\| + \left| P^{(t)} - P^{(t-1)} \right| \leq \epsilon_3$

**Output:**  $\hat{\mathbf{w}}^* = \mathbf{w}^{(t)}, \hat{P}^* = P^{(t)}, \hat{p}_1^*, \hat{p}_2^*$ .

---

### 3.3 Complexity Analysis

We can find that **Algorithm 2** solves the problem  $L_1(L_2 + L_3)$  times, where  $L_1, L_2, L_3$  denote the number of iterations of BCD, SCA and CCCP, respectively. Besides, CVX is used to solve (17) and its complexity is  $\mathcal{O}(L_2(2N + 2)^{3.5} \log(1/\epsilon))$ , where  $\mathcal{O}(\cdot)$  represents the big-O notation and  $\epsilon$  is the solution accuracy [12]. Then the computational complexity is  $\mathcal{O}(L_1(L_2(2N + 2)^{3.5} \log(1/\epsilon) + L_3))$ . By contrast, the complexity of **Algorithm 3** is  $\mathcal{O}(L_1(L_4 + L_3))$ , where  $L_4$  depends on the step size of the 1D search method. Obviously, **Algorithm 2** is more complicated than **Algorithm 3**.

## 4 Simulation Results

In this section, the performance for the mmWave-NOMA system with imperfect CSI is evaluated by computer simulation. For the simulation setup, it is assumed that the channel condition of User-1 is better than that of User-2. For the mmWave channel, we set  $L_i = 4, i = 1, 2$ , and the first channel path is line-of-sight path, where  $|\lambda_{1,1}| = 1, |\lambda_{2,1}| = 0.3, \cos(\theta_{1,1}) = -0.25, \cos(\theta_{2,1}) = 0.4$  and the rest are NLOS paths, where  $\lambda_{i,l} (l = 2, 3, 4) \in \mathcal{CN}(0, 10^{-15/10})$  and AoDs are uniformly distributed over  $[0, 2\pi]$ . The tolerances are  $\epsilon_1 = \epsilon_2 = \epsilon_3 = 10^{-4}$ . Other parameters are set as  $r_1 = r_2 = r = 1$  bit/s/Hz,  $N = 32, P_{BB} = 200$  mW,  $P_{RF} = 160$  mW,  $P_{PS} = 20$  mW,  $P_{LNA} = 40$  mW,  $\xi = 1/0.38, \sigma^2 = 1$  mW [7], where the computer used is equipped with Intel Core i5-6300HQ 2.30 GHz and 4 G RAM.

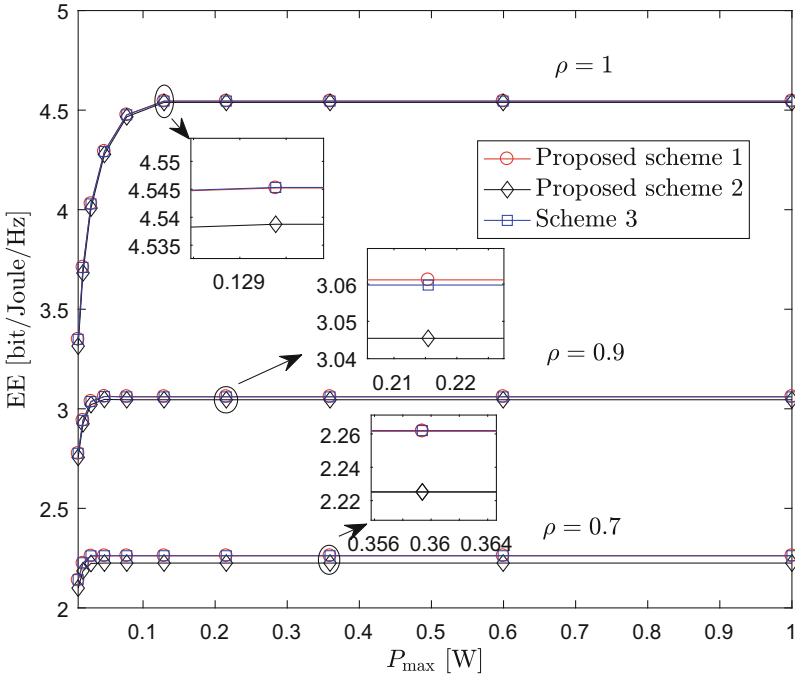


**Fig. 1.** Effect of imperfect CSI on the system EE under different schemes.

Figure 1 shows the system EE with different joint design schemes, including the BF design of “Proposed scheme 1” based on SCA and that of “Proposed scheme 2” based on 1D search method and “Scheme 3” that searches for the phase  $\delta_n (n = 1, \dots, N)$  of the  $n$ -th entry of  $\mathbf{w}$  over  $[0, 2\pi]$  corresponds to maximum  $J_3(\mathbf{w})$ , where  $\mathbf{w} = \frac{1}{\sqrt{N}} [e^{j\delta_0}, \dots, e^{j\delta_N}]$ . Moreover, “Scheme 3” uses  $N$  times

1D search which improves accuracy at the cost of efficiency. Obviously, the performance of both schemes is close to that of “Scheme 3”, and “Proposed scheme 1” outperforms “Proposed scheme 2”, while “Scheme 3” costs the most run time, followed by “Proposed scheme 1”, and “Proposed scheme 2” has the lowest complexity. Specially, the average run time of three schemes when  $\rho = 0.9$  is 5.1801 s, 0.4404 s and 17.2136 s, respectively and the result shows “Scheme 3” has the highest complexity because it requires  $N$  times 1D search method, and complexity of “Proposed scheme 1” is much more than that of “Proposed scheme 2” because CVX has poor computational efficiency, which results in longer run time. Besides, Fig. 1 presents the impact of imperfect CSI on the system EE, where  $\rho \in \{1, 0.9, 0.7\}$ . As can be observed, the system EE decreases along with the decrease of  $\rho$ , which concludes that the accuracy of channel estimation affects the EE significantly. This is because the channel estimation error results in the increase of interference when decoding the user’s signals.

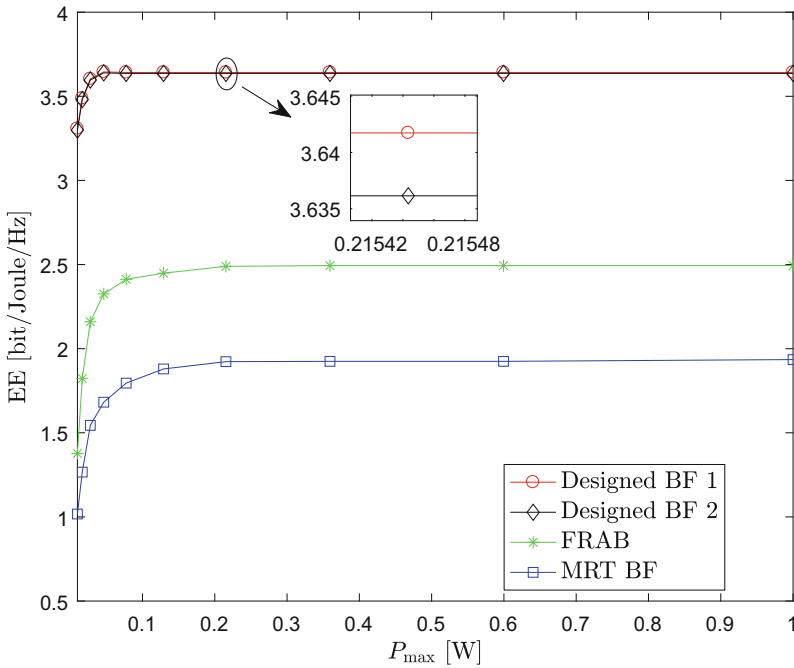


**Fig. 2.** EE performance of the mmWave-NOMA system under different BF schemes.

Figure 2 evaluates the EE performance with our proposed schemes and the finite resolution analog beamforming (FRAB) in [13], and maximal-ratio transmit (MRT) BF when  $\rho = 0.95$ ,  $r = 0.1$  bit/s/Hz, where “Designed BF 1” refers to SCA-based BF design, “Designed BF 2” refers to BF design based on 1D search, “FRAB” and “MRT BF” solve the PA problem under given BF. From Fig. 2,

the proposed schemes have better performance than the other two schemes, since the BF vectors of “FRAB” scheme and “MRT BF” scheme are independent and not optimized with PA jointly, which verifies the effectiveness of two proposed schemes.

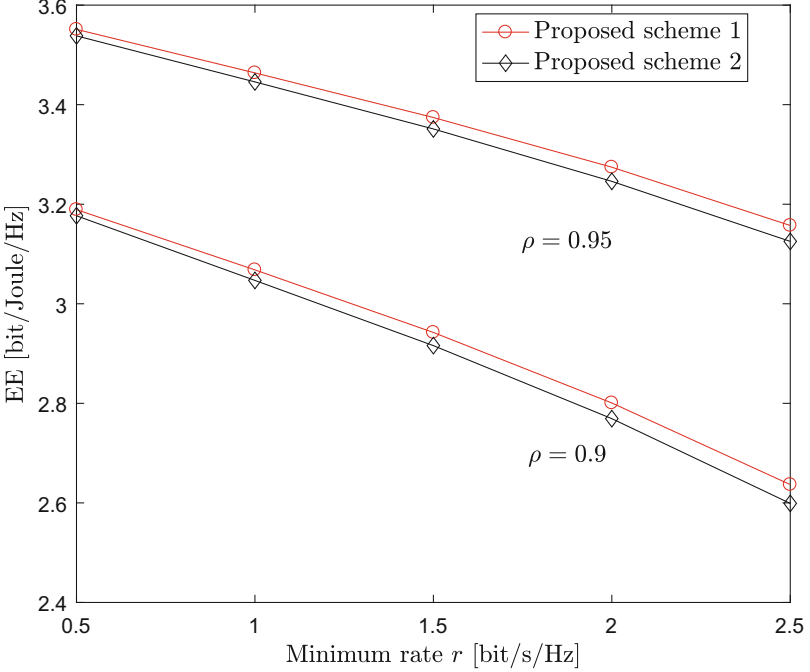


**Fig. 3.** EE comparison under different rate constraints.

Figure 3 plots the EE versus rate constraints with two schemes when  $\rho \in \{0.95, 0.9\}$  and  $P_{\max} = 1$  W. As shown in Fig. 3, the system EE declines with the minimum rates. And the higher the minimum rate, the more EE is reduced. This is because “Proposed scheme 2” is formulated without considering the rate constraint. The higher the minimum rate is, the more performance loss it will bring. Besides, the gap between two schemes is bigger with the increase of minimum rate, since the rate constraint has more effect on “Proposed scheme 2”.

## 5 Conclusion

This paper studies on the energy-efficient joint PA and BF design problem for downlink mmWave-NOMA system under imperfect CSI. The basic idea is to decompose the optimization problem into the PA problem and BF design problem, and then solve them in succession by BCD. Specifically, for the PA problem,

we derive the closed-form solution of CCCP by Lambert W function. For the BF design problem, we obtain a suboptimal solution by SCA and also derive a suboptimal beamforming utilizing the 1D search method. In the simulation, we analyze the effect of estimation error and rate constraints on the EE, respectively. The results prove the effectiveness of two proposed schemes. Moreover, the suboptimal scheme utilizing 1D search method can implement EE performance closing to that based on SCA and has better computational efficiency.

## References

1. Dai, L., Wang, B., Ding, Z., Wang, Z., Chen, S., Hanzo, L.: A survey of non-orthogonal multiple access for 5G. *IEEE Commun. Surv. Tutor.* **20**(3), 2294–2323 (2018). Thirdquarter
2. Zhu, L., Zhang, J., Xiao, Z., Cao, X., Wu, D.O., Xia, X.G.: Joint power control and beamforming for uplink non-orthogonal multiple access in 5G millimeter-wave communications. *IEEE Trans. Wirel. Commun.* **17**(9), 6177–6189 (2018)
3. Xiao, Z., Zhu, L., Choi, J., Xia, P., Xia, X.: Joint power allocation and beamforming for non-orthogonal multiple access (NOMA) in 5G millimeter wave communications. *IEEE Trans. Wirel. Commun.* **17**(5), 2961–2974 (2018)
4. Zeng, M., Hao, W., Dobre, O.A., Poor, H.V.: Energy-efficient power allocation in uplink mmWave massive MIMO with NOMA. *IEEE Trans. Veh. Technol.* **68**(3), 3000–3004 (2019)
5. Hao, W., Zeng, M., Chu, Z., Yang, S.: Energy-efficient power allocation in millimeter wave massive MIMO with non-orthogonal multiple access. *IEEE Wirel. Commun. Lett.* **6**(6), 782–785 (2017)
6. Hao, W., et al.: Codebook-based max-min energy-efficient resource allocation for uplink mmWave MIMO-NOMA systems. *IEEE Trans. Commun.* **67**(12), 8303–8314 (2019)
7. Yu, X., Dang, X., Wen, B., Leung, S., Xu, F.: Energy-efficient power allocation for millimeter-wave system with non-orthogonal multiple access and beamforming. *IEEE Trans. Veh. Technol.* **68**(8), 7877–7889 (2019)
8. Wei, Z., Ng, D.W.K., Yuan, J.: NOMA for hybrid mmWave communication systems with beamwidth control. *IEEE J. Sel. Top. Sig. Process.* **13**(3), 567–583 (2019)
9. Guo, J., Yu, Q., Meng, W., Xiang, W.: Energy-efficient hybrid precoder with adaptive overlapped subarrays for large-array mmWave systems. *IEEE Trans. Wirel. Commun.* **19**(3), 1484–1502 (2020)
10. Hoorfar, A.: Inequalities on the Lambert W function and hyperpower function. *J. Inequal. Pure Appl. Math.* **9**(2), 5–9 (2013)
11. Grant, M., Boyd, S.: CVX: MATLAB software for disciplined convex programming, Version 2.2, January 2020. <http://cvxr.com/cvx>
12. Ben-Tal, A., Nemirovski, A.: Lectures on Modern Convex Optimization: Analysis, Algorithms, and Engineering Applications. SIAM Series Optimization, vol. 2, November 2001
13. Dai, L., Wang, B., Peng, M., Chen, S.: Hybrid precoding-based millimeter-wave massive MIMO-NOMA with simultaneous wireless information and power transfer. *IEEE J. Sel. Areas Commun.* **37**(1), 131–141 (2019)